Predictive Biomarkers and Personalized Medicine

Clinical Cancer Research

FGFR2 Gene Amplification in Gastric Cancer Predicts Sensitivity to the Selective FGFR Inhibitor AZD4547

Liang Xie[1], Xinying Su[1], Lin Zhang[1], Xiaolu Yin[1], Lili Tang[1], Xiuhua Zhang[1], Yanping Xu[1], Zeren Gao[1], Kunji Liu[1], Minhua Zhou[1], Beirong Gao[1], Danping Shen[2], Lianhai Zhang[3], Jiafu Ji[3], Paul R. Gavine[1], Jingchuan Zhang[1], Elaine Kilgour[4], Xiaolin Zhang[1], and Qunsheng Ji[1]

Abstract

Purpose: *FGFR* gene aberrations are associated with tumor growth and survival. We explored the role of *FGFR2* amplification in gastric cancer and the therapeutic potential of AZD4547, a potent and selective ATP-competitive receptor tyrosine kinase inhibitor of fibroblast growth factor receptor (FGFR)1–3, in patients with *FGFR2*-amplified gastric cancer.

Experimental Design: Array-comparative genomic hybridization and FISH were used to identify *FGFR2* amplification in gastric cancer patient tumor samples. The effects of FGFR2 modulation were investigated in gastric cancer cells with *FGFR2* amplification and in patient-derived gastric cancer xenograft (PDGCX) models using two approaches: inhibition with AZD4547 and short hairpin RNA (shRNA) knockdown of *FGFR2*.

Results: Amplification of the *FGFR2* gene was identified in a subset of Chinese and Caucasian patients with gastric cancer. Gastric cancer cell lines SNU-16 and KATOIII, carrying the amplified *FGFR2* gene, were extremely sensitive to AZD4547 *in vitro* with GI_{50} values of 3 and 5 nmol/L, respectively. AZD4547 effectively inhibited phosphorylation of FGFR2 and its downstream signaling molecules and induced apoptosis in SNU-16 cells. Furthermore, inhibition of FGFR2 signaling by AZD4547 resulted in significant dose-dependent tumor growth inhibition in *FGFR2*-amplified xenograft (SNU-16) and PDGCX models (SGC083) but not in nonamplified models. shRNA knockdown of *FGFR2* similarly inhibited tumor growth *in vitro* and *in vivo*. Finally, compared with monotherapy, we showed enhancement of *in vivo* antitumor efficacy using AZD4547 in combination with chemotherapeutic agents.

Conclusion: FGFR2 pathway activation is required for driving growth and survival of gastric cancer carrying *FGFR2* gene amplification both *in vitro* and *in vivo*. Our data support therapeutic intervention with FGFR inhibitors, such as AZD4547, in patients with gastric cancer carrying *FGFR2* gene amplification. *Clin Cancer Res; 19(9); 2572–83. ©2013 AACR.*

Introduction

Gastric cancer is the second leading cause of death from cancer worldwide and accounts for nearly 1 in 10 of all cancer deaths (1). Most new cases and deaths occur in East Asian countries, including China, Japan, and Korea (2). Such high incidence rates in this region may be due in part to the preference for a high-salt diet, a high proportion of smokers, and a high prevalence of *Helicobacter pylori* infection (2, 3). Despite advances in diagnostic methods and improvement of both surgical skills and systematic chemotherapy regimens, the overall prognosis for gastric cancer remains disappointing, especially for those with late-stage disease; the 5-year survival rate for patients with stage III/IV metastatic gastric cancer is only around 10% (4, 5). Better management of this disease, particularly through the use of targeted therapeutic agents, is required.

Genetic abnormality and intratumor heterogeneity are 2 typical features of cancer cells, which play crucial roles in carcinogenesis and tumor progression (6). Although detailed mechanisms of tumor development driven by gene amplification, mutation, or translocation have not been fully characterized (7), aberrant genes have been shown clinically as valid targets for cancer treatment (8–10). A key challenge that remains, however, is how to distinguish these

Authors' Affiliations: [1]Innovation Center China, AstraZeneca R&D; [2]Renji Hospital, School of Medicine, Shanghai Jiao Tong University, Shanghai; [3]Department of Surgery, Peking University Cancer Hospital, Beijing Institute for Cancer Research, Key laboratory of Carcinogenesis and Translational Research (Ministry of Education), Beijing, China; and [4]AstraZeneca Oncology, Macclesfield, Cheshire, United Kingdom

Note: Supplementary data for this article are available at Clinical Cancer Research Online (http://clincancerres.aacrjournals.org/).

L. Xie and X. Su contributed equally to this work.

Corresponding Author: Qunsheng Ji, Innovation Center China, AstraZeneca, Building 7, 898 Halei Road, Zhangjiang Hi-Tech Park, Shanghai 201203, China. Phone: 86-2161097882; Fax: 86-2161097722; E-mail: Qunsheng.Ji@astrazeneca.com

doi: 10.1158/1078-0432.CCR-12-3898

Translational Relevance

Amplification of the *FGFR2* gene may be involved in oncogenesis and progression of gastric cancer. This report describes the incidence of *FGFR2* amplification in gastric cancer and a preclinical assessment of the therapeutic potential of AZD4547, a selective fibroblast growth factor receptor (FGFR) kinase inhibitor. Following identification of *FGFR2* gene amplification in a subgroup of Chinese and Caucasian patients with gastric cancer, the dependency of FGFR2 signaling (activated by *FGFR2* amplification) for gastric tumor growth and survival, both *in vitro* and *in vivo*, was systematically shown. AZD4547 treatment resulted in tumor regression in gastric cancer xenografts derived from patients carrying *FGFR2* gene amplification, but not in nonamplified models. Regression was accompanied by inhibition of phospho-FGFR2 and downstream pathway inactivation. The comprehensive translational studies presented here support a tumorigenic role for *FGFR2* gene amplification in patients with gastric cancer and warrant clinical investigation of FGFR inhibitors, including AZD4547, in this setting.

so-called "driver" oncogenes from other coexisting "passenger" genes (11). To facilitate the identification and validation of "driver" genes, patient-derived specimen-based molecular analysis techniques and *in vivo* disease models have been widely used (12–14). Consequently, a number of candidate oncogenes, including several within the receptor tyrosine kinase (RTK)/RAS pathway, have been discovered in gastric cancers (15, 16).

Fibroblast growth factor receptor family members (FGFR1–4) belong to the RTK superfamily. Through interaction with FGF ligands, the receptors are involved in diverse cellular functions including regulation of development processes, mediation of cell proliferation and differentiation, as well as angiogenesis and tissue regeneration (17–19). Binding of the FGF ligand to the receptor induces dimerization of the FGF:FGFR complex, leading to kinase activation and autophosphorylation of multiple tyrosine residues in the cytoplasmic domain of the receptor. This results in activation of downstream signaling of the phosphoinositide 3-kinase (PI3K)-AKT and mitogen-activated protein kinase–extracellular signal–regulated kinase (MAPK-ERK) pathways (20). Genetic modifications or overexpression of FGFRs have been associated with tumorigenesis and progression in breast, prostate, stomach, and hematologic malignancies (21, 22). In particular, abnormal activation of FGFR2 signaling has been linked with several types of human cancers, and somatic *FGFR2* mutations have been reported in lung, gastric, and ovarian cancers (23–25). *FGFR2* amplification has been associated with tumor cell proliferation and survival of gastric cancer cell lines (26). Furthermore, *FGFR2* amplification may correlate with a poor prognosis for patients with gastric cancer (27). Thus, FGFR2 has attracted significant attention as a potential therapeutic candidate for the development of targeted therapeutic anticancer agents (28).

AZD4547 is an orally bioavailable, highly selective, and potent ATP-competitive small-molecule tyrosine kinase inhibitor of FGFR1–3. We have previously described the chemical structure and selectivity profile of this compound and shown that it can significantly inhibit FGFR phosphorylation and repress proliferation of cancer cell lines via inhibition of FGFR signaling (29). AZD4547 treatment has also exhibited antitumor activity in a representative FGFR-driven human tumor xenograft model. Currently, the compound is under investigation in several phase I and II clinical trials (ClinicalTrials.gov identifiers: NCT01202591; NCT01457846; NCT00979134; NCT01213160).

In the current study, amplification of the *FGFR2* gene was identified in a subset of Chinese and Caucasian patients with gastric cancer. Subsequently, we aimed to investigate the preclinical activity of AZD4547 in *FGFR2*-amplified gastric cancer models and ultimately showed potent antitumor activity with tumor regression selectively occurring in *FGFR2*-amplified gastric cancer xenografts.

Materials and Methods

Materials

The following chemical reagents were all obtained from Sigma-Aldrich: cisplatin (Cat# P4394), fluorouracil (Cat# F6627), docetaxel (Cat# 01885), and irinotecan (Cat# I1406).

The following antibodies were purchased from Cell Signaling Technology: phospho-FGFR2 (tyr653/654), phospho-FRS2α (tyr436), phospho-PLCγ 1 (Tyr783), phospho-p44/p42 MAPK (Erk1/2), total-Erk, phospho-S6 (ser240/244), total-S6, cleaved caspase-3, PARP, and horseradish peroxidase (HRP)-linked anti-rabbit immunoglobulin G (IgG). Other antibodies included total-FRS2 (R&D Systems), total-FGFR2 (Abcam), phospho-PLCγ (tyr783; Epitomics), and Ki67 (Dako). An antibody against β-actin (Sigma) was used as a control.

A panel of 29 gastric cancer cell lines was obtained from the American Type Culture Collection or from internal collections. SNU-16 cells were maintained in RPMI-1640 medium supplemented with 10% FBS (Invitrogen) and 2 mmol/L L-glutamine (Invitrogen). All cell lines were genetically tested and authenticated using the StemElite ID System Kit (Promega, #G9530) and were not cultured for more than 3 months before conducting the work described here.

Female Balb/c nude mice of ages 6- to 8-week-old and 8- to 10-week-old female (nu/nu) severe combined immunodeficient mice (SCID) nude mice were purchased from Vital River. Animals were housed in a specific pathogen-free animal facility in accordance with the Guide for Care and Use of Laboratory Animals (eighth edition) and the regulations of the Institutional Animal Care and Use Committee (IACUC). All animal studies were approved by the IACUC.

All studies using human tissues were conducted with the patients' consent and the approval of the Local Research Ethics committee.

Array comparative genomic hybridization analysis of gastric cancer patient samples

FGFR2 gene copy number was analyzed in frozen patient tissue samples using the Agilent 244K array comparative genomic hybridization (aCGH) platform. The quality of the raw data was checked with Agilent CGH Analytics software, using the derivative of the log ratio spread (DLRSpread) as a surrogate for assay quality. Any sample with a DLRSpread more than 0.3 was excluded from further analysis. Data for those samples that qualified for further assessment were subsequently analyzed using Nexus software (version 4) for recovery of *FGFR2* segmental structure (segmentation) and the discrete copy number value at the single-sample level (calling). Segments with an aCGH log ratio (copy number of sample vs. control) more than 0.8, were classified as amplified.

FISH analysis

The *FGFR2* FISH probe was generated from BAC (RP11-62L18) DNA directly labeled with Spectrum Red (ENZO, #02N34-50). The Spectrum Green-labeled centromere of chromosome 10 (CEP10) probe (Vysis #32-132010) was used as an internal control. FISH analysis was conducted according to routine methodology (30). In brief, 4-μm sections from formalin-fixed and paraffin-embedded (FFPE) gastric cancer patient tissue samples were deparaffinized. After pretreatment with the SpotLight Tissue pretreatment Kit (Invitrogen, #00-8401), tissue sections and the *FGFR2*/CEP10 probes were denatured at 80°C for 5 minutes, and then incubated together at 37°C for 48 hours. Following this hybridization step, excess and unbound probes were removed with posthybridization wash buffer (0.3% NP40/1× saline-sodium citrate at 75.5°C for 5 minutes followed by 2 washes of 2× saline-sodium citrate at room temperature for 2 minutes), and nuclei were counterstained with 4′,6 diamidino-2-phenylindole (DAPI). Visualization of the fluorescent signals was conducted using a fluorescence microscope (Olympus) equipped with appropriate filters and image analysis was conducted with CytoVision (Leica). The enumeration of the *FGFR2* gene and chromosome 10 was conducted in 50 tumor nuclei for each tissue section. Amplification of *FGFR2* was defined as a *FGFR2*:chromosome 10 ratio of $\geq$2, or tight *FGFR2* gene clusters in $\geq$10% of the nuclei analyzed per tissue section.

Immunohistochemistry

Immunohistochemical (IHC) analysis was conducted using a Lab Vision autostainer. In brief, 3-μm FFPE sections were dewaxed and rehydrated on the Leica XL autostainer and underwent antigen retrieval for 5 minutes in pH 6 retrieval buffer (S1699; Dako) followed by washing in running tap water for 5 minutes. Sections were rinsed in Tween–TBS (TBST) and incubated with endogenous peroxidase block for 10 minutes. Slides were washed in TBST and then incubated with primary antibodies: phospho-Erk (Cell Signaling Technology, #4376; 1:50) or phospho-S6 (Cell Signaling Technology, #2215; 1:100) for 60 minutes at room temperature and finally washed in TBST twice. Slides were reacted with EnVision+ System-HRP Labeled Polymer Anti-rabbit for 30 minutes and washed in TBST twice, developed in diaminobenzidine substrate for 5 minutes, and rinsed in tap water. Sections were counterstained, dehydrated, and cleared in Leica XL autostainer, and finally sealed in the ClearVue automated cover slipper. Normal rabbit IgG (Dako, X9003) at 1:18,000 and 1:20,000 dilution was used as negative control for phospho-ERK and phospho-S6, respectively. For IHC detection of the proliferation marker Ki67, FFPE sections were pretreated with an Animal Research Kit (Dako, K3954) according to manufacturer's instructions. Sections were then incubated with anti-Ki67 primary antibody (Dako, M7240; 1:100) for 15 minutes at room temperature, and washed twice in TBST, followed by incubation with streptavidin-peroxidase for 15 minutes, washed twice in TBST, counterstained with DAPI, and visualized by chemiluminescence, as described earlier. To evaluate apoptotic cell death within the xenografts, TUNEL assay was conducted on xenograft sections using the *In Situ* Cell Death Detection Kit (Roche, 12156792910) according to the manufacturer's instructions.

In vitro antiproliferative cell panel screening

All 29 gastric cancer cell lines were seeded at optimized density in 96-well culture plates. Adherent cells were seeded the night before the start of treatment; suspension cells were seeded concurrently with treatment. Cells were treated with AZD4547 for 72 hours at concentrations ranging from 0 to 30 μmol/L. Control cells were treated with dimethyl sulfoxide (DMSO) only. Cell proliferation was measured using the CellTiter 96 Aqueous One Solution Cell Proliferation Assay Kit (Promega), according to the manufacturer's instructions. Evaluation of cell proliferation of SNU5 and SNU16 cells was conducted using AlamarBlue Proliferation Assay Kit (Invitrogen), an assay with a similar detection mechanism and a better signal window.

In vitro pharmacodynamics study

SNU-16 or KATO-III cells were seeded at a density of 2×10^5 cells/mL in RPMI-1640 medium containing 10% FBS and cultured overnight. The cells were then incubated with AZD4547 0.001, 0.003, 0.01, 0.03, or 0.1 μmol/L for 1 hour before being lysed in cell lysis buffer (Cell Signaling Technology) containing phosphatase and protease inhibitors (Sigma) and then 20 μg of protein was loaded onto 4% to 12% (w/v) NuPAGE gels; following electrophoresis, the lysates were transferred to polyvinylidene difluoride (PVDF) membranes and probed with the following antibodies: phospho-FGFR (tyr653/654; Cell Signaling Technology, #3471; 1:1,000), phospho-FRS2 (tyr436; Cell Signaling Technology, #3861; 1:1,000), phospho-PLCγ (tyr783; Epitomics, #2325-1; 1:1,000), phosphor-p44/p42 MAPK (Erk1/2; Cell Signaling Technology, #4370) or phospho-S6 (ser240/244; Cell Signaling Technology,

#2215; 1:1,000). The appropriate secondary antibody was applied and visualization was conducted using SuperSignal West Dura chemiluminescence substrate (Pierce) according to the manufacturer's instructions. Membranes were reprobed to assess total-Erk1/2 (Cell Signaling Technology, #4960) and total-S6 levels (Cell Signaling Technology, #2317; 1:1,000).

In vitro cell-cycle analysis study

SNU-16 cells were exposed to AZD4547 0 (DMSO control), 3, 10, or 30 nmol/L for 48 hours. For fluorescence-activated cell sorting (FACS), cells were washed with PBS and then incubated with staining solution containing 0.2 mg/mL RNase A (Fermentas), 0.05 mg/mL propidium iodide (Invitrogen) and 0.1% Triton (Sigma) in PBS for 20 minutes at room temperature. Then cell-cycle distributions were assessed with a FACSCanto instrument (BD).

Establishment of standard gastric cancer xenograft and patient-derived gastric cancer xenograft mouse models

SNU-16 cancer cells (5×10^6) were suspended in 200 μL of 50% Matrigel and inoculated subcutaneously on either sides of the flank of balb/c nude mice. Once the volume of the tumor xenograft reached approximately 300 to 500 mm^3, it was excised and cut into approximately 2 mm^3 segments, which were further implanted subcutaneously via Trocar needle into nude mice.

Patient-derived gastric cancer xenograft (PDGCX) mouse models were generated using tumor tissue from Chinese patients with gastric cancer. In brief, surgically excised tumor tissue (F0) was cut into approximately 2 mm^3 segments and implanted subcutaneously into immune-compromised nude mice or SCID mice (F1). Transplantation occurred within 2 hours following excision. Subsequent passages were made into additional nude mice once the grafted tumors had reached a size of 400 to 600 mm^3. PDGCX models within 10 passages (between F3 to F10) were used to evaluate antitumor efficacy.

For all *in vivo* studies, tumors were measured in 2 dimensions with calipers and the tumor volume was calculated using the following formula: tumor volume = (length × width^2) × 0.5.

In vivo antitumor efficacy studies

SNU-16 xenograft model and PDGCX mouse models were used to study the efficacy of AZD4547. For single-agent studies, mice were randomized into groups of 8 when tumor xenograft volumes reached 150 to 250 mm^3, and treated with either control vehicle (DMSO) or AZD4547 at doses ranging from 1.56 to 25 mg/kg, administered orally, once daily for several weeks. For combination studies with chemotherapy, animals were treated with low doses of AZD4547 3.125 mg/kg/qd, either alone, or in combination with FC [5-fluorouracil (5-FU) 10 mg/kg/once daily plus cisplatin 4 mg/kg/once weekly], docetaxel 3 mg/kg/once weekly, irinotecan 17.5 mg/kg/once weekly, or control vehicle (1% Tween 80, 5-FU 10 mg/kg/once daily, 5 days on, 2 days off treatment). The doses of cytotoxic agents were based on the clinically recommended dosage for human use. Tumor volume and body weight of the mice were measured twice weekly.

In vivo single dose pharmacodynamics study and pharmacokinetics/pharmacodynamics modeling

SNU-16 tumor-bearing mice were administered a single oral dose of AZD4547 12.5 mg/kg once the tumor volume reached 400 to 500 mm^3. Plasma and xenograft tissue samples were collected from each animal at the following time points post-dose: 0, 1, 2, 4, 8, and 24 hours. The total plasma concentration of AZD4547 was determined by liquid chromatography/mass spectrometry (LC/MS) methods. Each xenograft tissue sample was divided into 2: one half underwent formalin fixation for IHC analysis and the other half was for snap-frozen in liquid nitrogen. Phospho-FGFR and phospho-PLCγ expression levels for the pharmacokinetics/pharmacodynamics correlation study were determined by Western blot analysis on snap-frozen samples and phospho-Erk expression was determined by IHC analysis on formalin-fixed samples (phospho-FGFR, Cell Signaling Technology, #3471; 1:1,000; phospho-Erk, Cell Signaling Technology, #4370; 1:1,000; phospho-PLCγ, Cell Signaling Technology, #2821; 1:1,000).

The PDGCX-based pharmacodynamics study was conducted on xenograft tissue samples derived from animals treated as part of the AZD4547 efficacy study. Mice that had previously been administered AZD4547 1.56 mg/kg/once daily during the efficacy study were given a single dose of AZD4547 12.5 mg/kg. Two hours post-dose, xenograft tissue samples were collected and formalin-fixed sections were probed for phospho-Erk and phospho-S6 levels using IHC methods described earlier.

Inducible shRNA knockdown of *FGFR2 in vitro* and *in vivo*

A construct containing *FGFR2*-specific (exon 17) short hairpin RNA (shRNA) sequence under the control of the tetracycline promoter was used for this study. The shRNA sequences were 2B: GAATGAAGAACACGACCAA and 3C: GACTTGGATCGAATTCTCA (Invitrogen). SNU-16 cells were transfected with the *FGFR2* construct and stable clones were selected using the antibiotic puromycin (Sigma-Aldrich; P9620). A construct containing enhanced GFP (*EGFP*)-specific shRNA sequence was used as a control, in which expression of shRNA can be induced by doxycycline (Sigma-Aldrich; D9891). SNU-16 parental cells and 4 stable clones (SNU-16_sh-EGFP control, SNU-16_sh-FGFR2 2B, SNU-16_sh-FGFR2 3C6, and SNU-16_sh-FGFR2 3C8) were established and used for the *FGFR2* knockdown studies.

For the *in vitro* study, SNU-16 cells were treated with doxycycline 1 μg/mL for 1, 2, or 4 days, and the levels of FGFR2, phospho-FGFR, and cleaved caspase-3 in the cell lysates were determined by Western blot analysis.

For the *in vivo* study, xenografts from stable clones SNU-16_sh-EGFP control, SNU-16_sh-FGFR2 2B, and SNU-16_sh-FGFR2 3C8 were established following the methods described earlier. For each established xenograft, 2 small

fragments (approximately 15 mm^3) were implanted subcutaneously with 50% Matrigel into the right flank of balb/c nude mice. Mice bearing tumors with volumes approximating 150 to 250 mm^3 were randomized into 2 groups, with 8 mice per group. For mice receiving treatment, doxycycline was dissolved in 5% sucrose solution to a working concentration of 2 mg/mL and administered via the drinking water, which was protected from light and replaced every 2 to 3 days. Control groups received drinking water with 5% sucrose solution only. Treatment duration was 2 weeks for SNU-16_sh-FGFR2 2B-implanted mice and 3 weeks for SNU-16 parental, SNU-16_sh-FGFR2 3C8, and SNU-16_sh-EGFP mice.

Results

FGFR2 is genetically amplified in tumor samples from patients with gastric cancer

Tumor samples for aCGH analysis were provided by the Beijing Cancer Hospital (Beijing, China). Eligible samples (tumor content of $\geq$70%) were collected from 131 Chinese patients with gastric cancer; the median age of the patients was 62 years (range, 34–81) and the majority were male ($n = 94$; 71%). Twenty age-matched tumor-free samples were used as control tissue. Amplification of the *FGFR2* gene was identified in 3 (2%) of the 131 samples analyzed (Fig. 1A).

For FISH analysis, 197 Chinese gastric cancer patient samples were provided by the Renji Hospital [Shanghai, China; median age 62 years (range, 17–87); male $n = 133$ (67.5%)]. In addition, 97 Caucasian gastric cancer patient samples were also analyzed [78 tissue microarray samples (TriStar technology) and 19 samples from the AstraZeneca Biobank; median age 67 years (range, 38–93); male $n = 66$ (68%)]. *FGFR2* amplification was identified in 9 (5%) of 197 samples from Chinese patients and 7 (7%) of 97 samples from Caucasian patients (Supplementary Table S1). Representative *FGFR2*-amplified and control FISH images are shown in Fig. 1B.

FGFR2-amplified gastric cancer cell lines are hypersensitive to AZD4547 treatment

Of 29 human gastric cancer cell lines screened, 2 *FGFR2*-amplified human gastric cancer cell lines, KATO-III and SNU-16, exhibited extreme sensitivity to AZD4547 treatment, with GI_{50} values of 3 and 5 nmol/L, respectively. The remainder of the cell lines screened (all non-*FGFR2*-amplified), showed insensitivity to AZD4547 with GI_{50} values ranging from 1.6 to 30 μmol/L (Fig. 2A).

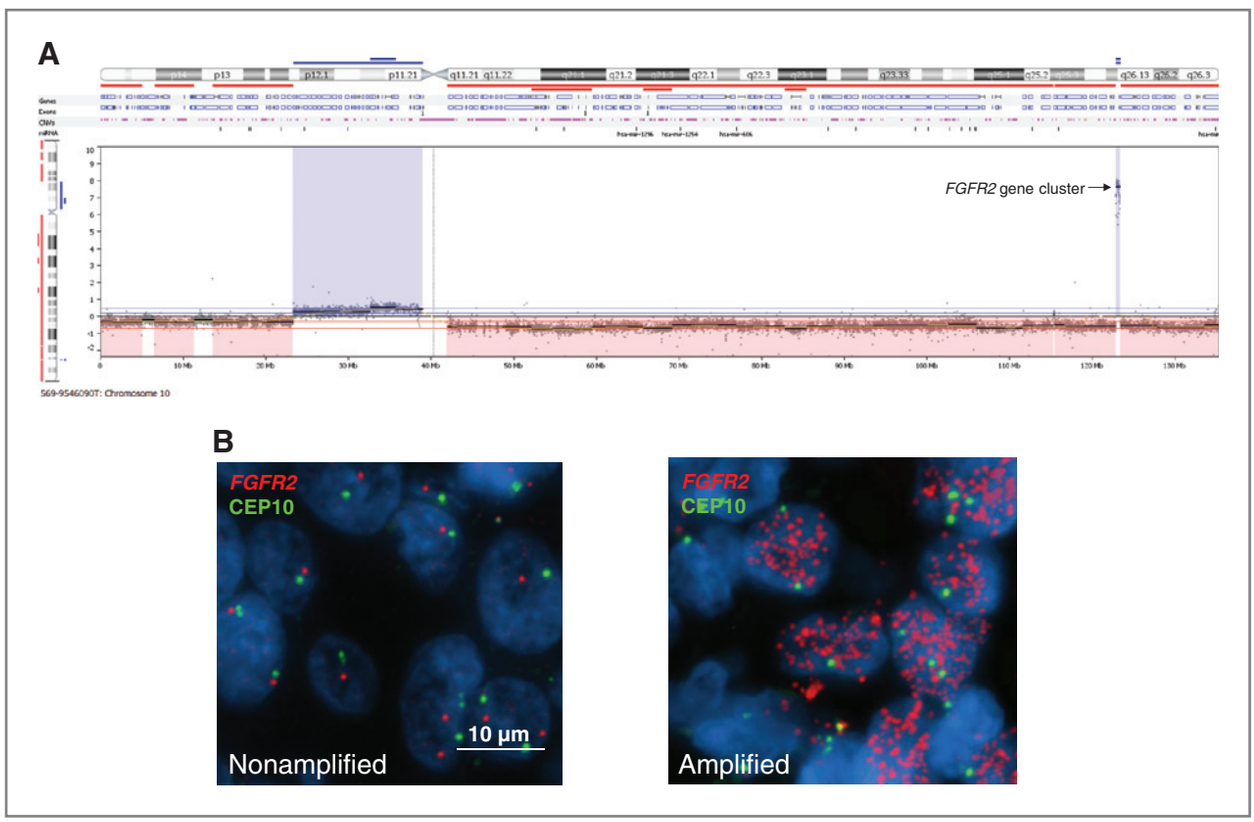

Figure 1. *FGFR2* gene amplification in Chinese and Caucasian gastric cancer patient samples. A, representative example of *FGFR2* gene amplification in a gastric tumor from a Chinese patient detected by aCGH ($n = 131$). B, representative example of focal *FGFR2* gene amplification from a cohort of Chinese gastric cancer specimens ($n = 197$) detected by FISH analysis. Left, a nonamplified sample; right, an amplified sample. Red signals represent *FGFR2* genes, whereas green signals are *CEP10*.

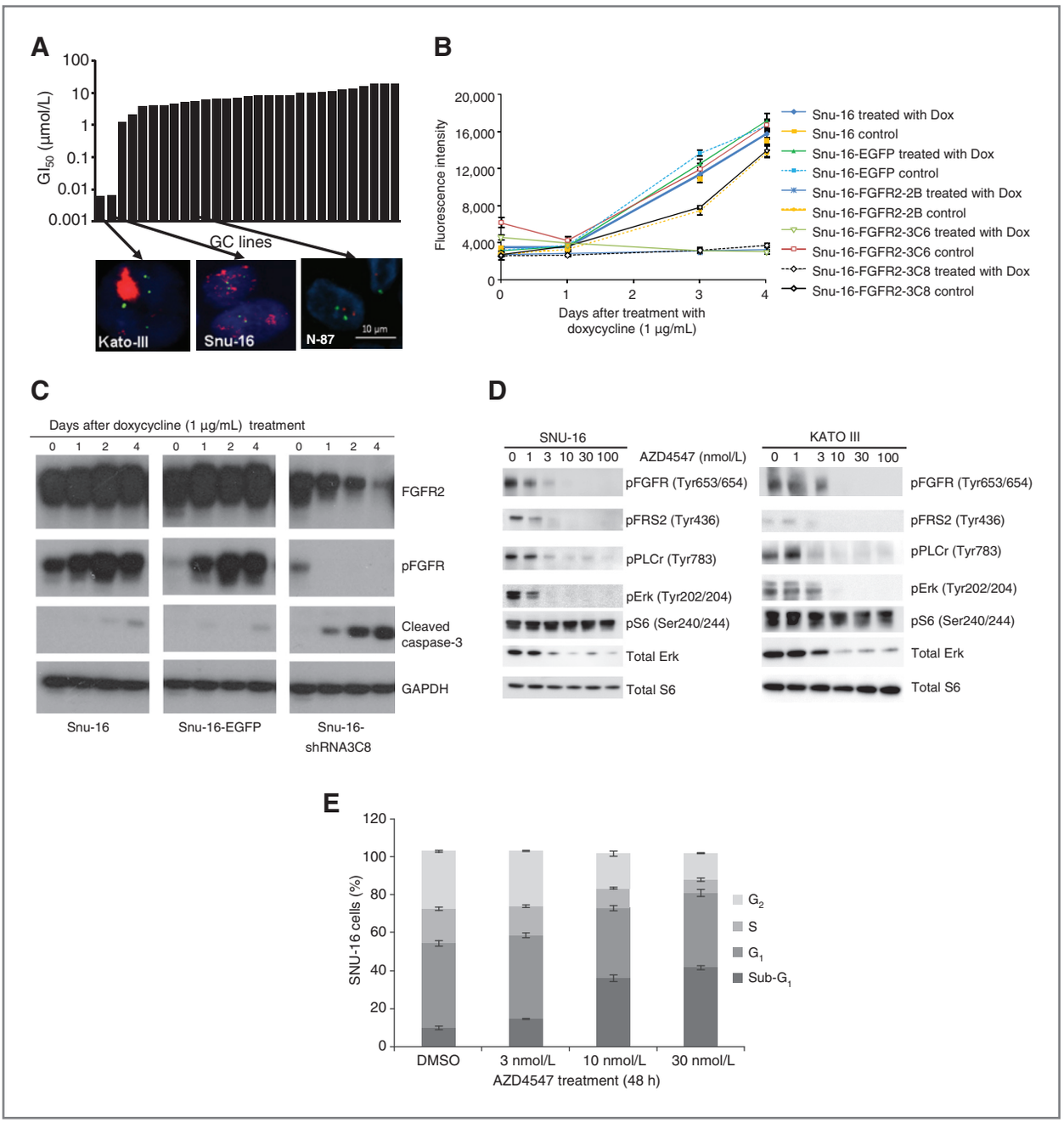

Figure 2. Validation of *FGFR2* gene amplification as an oncogenic driver in SNU-16 cells using pharmacologic and shRNA approaches. A, AZD4547 sensitivity correlates with *FGFR2* gene amplification status. *In vitro* MTS proliferation assay across a panel of 29 gastric cancer (GC) cell lines (top) showed that KATOIII and SNU16 cells were extremely sensitive to AZD4547, with GI_{50} values of 3 and 5 nmol/L, respectively. *FGFR2* gene copy number in these 2 cell lines was confirmed by FISH (bottom); both sensitive cell lines, KATOIII and SNU-16, showed strong *FGFR2* gene amplification, whereas AZD4547 insensitive lines (e.g., N-87), which were not *FGFR2*-amplified, had normal *FGFR2* gene status. B, *in vitro* growth curve of SNU-16 cells stably expressing 2 *FGFR2* specific shRNAs (1 clone for 2B; 2 clones for 3C, 3C6, and 3C8), vector control (EGFP), or untreated (SNU-16) with/without doxycycline (Dox) treatment. C, inducible knockdown of *FGFR2* by shRNA3C8 in SNU-16 cells resulted in a decrease of FGFR2 expression and FGFR2 phosphorylation compared with parental (SNU-16) or EGFP (vector control)–transfected cells after doxycycline treatment. Increased caspase-3 cleavage was observed following shRNA treatment. D, inhibition of FGFR2 pathway activation in the AZD4547-sensitive cell lines SNU-16 and KATOIII. Cells were incubated with AZD4547 at the indicated doses. Cell lysates were immunoblotted for phospho-FGFR, phospho-FRS2, phospho-PLCγ, phospho- and total-Erk, and phospho- and total-S6. E, the mechanism of *in vitro* growth inhibition by AZD4547 in *FGFR2*-amplified SNU-16 cells. SNU-16 cells were incubated with increasing concentrations of AZD4547 for 48 hours. Cell-cycle distribution was analyzed using propidium iodide and a FACSCanto flow cytometric system. GAPDH, glyceraldehyde-3-phosphate dehydrogenase.

AZD4547 modulation of FGFR2 signaling and shRNA knockdown of FGFR2 expression independently result in apoptotic induction in gastric cancer cells *in vitro*

To validate a role for *FGFR2* amplification and expression in driving tumorigenesis within gastric cancer cell lines, shRNA technology was used to modulate *FGFR2* expression. Stably expressing inducible shRNA SNU16 cell line clones were generated and tested in an *in vitro* proliferation assay. *FGFR2* knockdown potently inhibited the growth of SNU-16 gastric cancer cells *in vitro* (Fig. 2B). Following transfection with the construct incorporating *FGFR2* clone 3C8, total-FGFR2 levels were reduced in a time-dependent manner following doxycycline treatment, with phospho-FGFR2 being undetectable after 1 day. Importantly, cleaved caspase-3 levels were substantially increased under the same conditions (Fig. 2C). In contrast, both total- and phospho-FGFR2 were increased in parental or EGFP (vector control)–transfected SNU-16 cells after doxycycline treatment (Fig. 2C). Similar results were obtained with the control clone 3C6 (data not shown).

Following incubation with 30 nmol/L AZD4547, levels of phosphorylated FGFR2 and its downstream signaling molecules; PLCγ, FRS2, pErk1/2, and S6 were all reduced in SNU-16 cells and similar modulation of these phospho-markers was observed in the KATOIII cell line (Fig. 2D). Furthermore, dose-dependent increases in sub-G_1 population of SNU-16 cells were also detected at 48 hours post-AZD4547 treatment (Fig. 2E).

FGFR2 inhibition leads to tumor regression in SNU-16 xenografts *in vivo*

To extend the findings above, stable SNU-16 cell tet-controlled *FGFR2* expression clones were used in *in vivo* studies. Doxycycline treatment of mice harboring

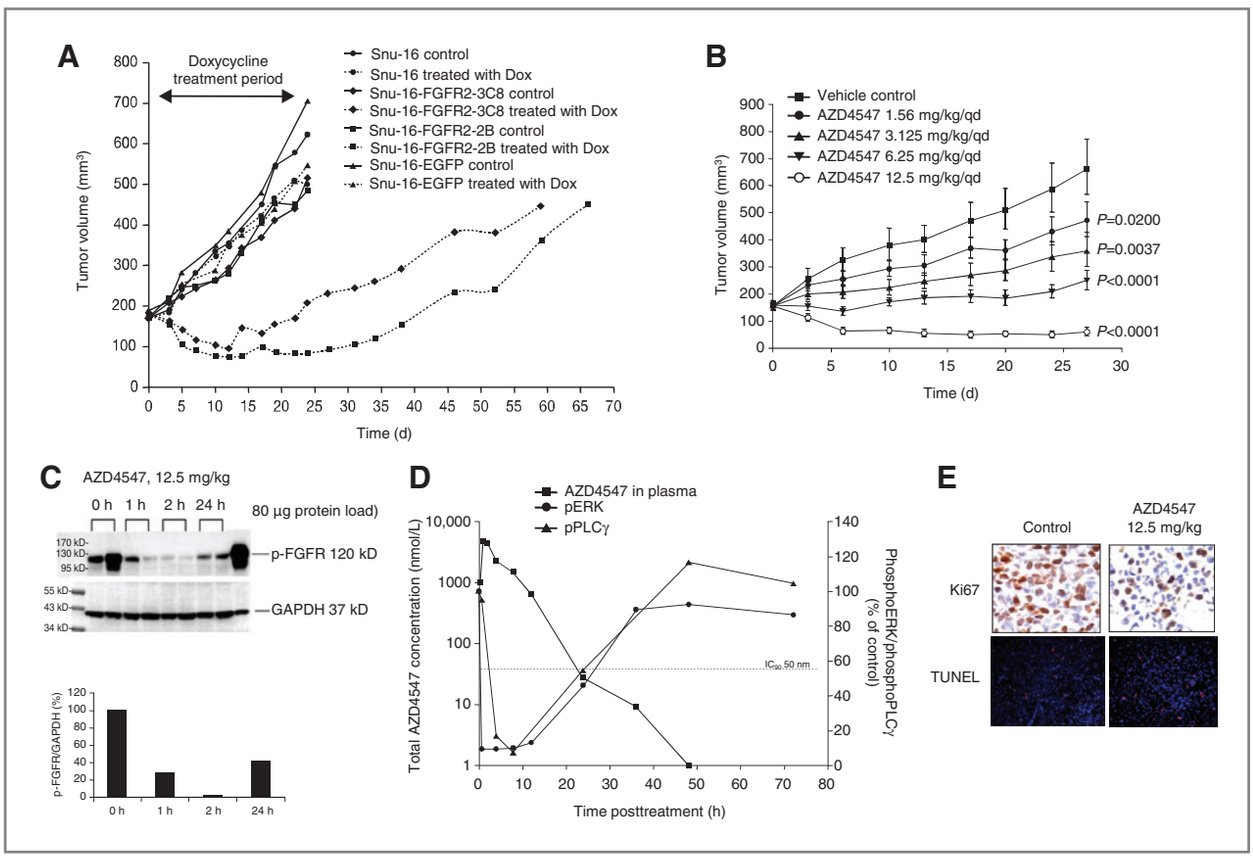

Figure 3. AZD4547 treatment leads to tumor regression in *FGFR2*-amplified SNU-16 gastric cancer xenografts. A, effect of *FGFR2* shRNA treatment on growth of SNU-16 xenografts *in vivo*. SNU-16 xenografts developed from cells carrying either stably expressing tet-controlled *FGFR2* shRNA (SNU16-ShRNA3C8 or 2B), EGFP control (SNU16-ShEGFP), or parental control (SNU16) were randomized into 2 groups and treated with/without doxycycline (Dox) 2 mg/mL in 5% sucrose solution. B, effect of AZD4547 treatment on tumor growth in the SNU-16 xenograft model. AZD4547 was administered by oral gavage once daily to nude mice bearing established subcutaneous SNU-16 xenografts at the doses indicated. Statistical analysis of TGI was conducted using a Student *t* test. C, analysis of SNU-16 xenograft tumor phospho-FGFR levels following AZD4547 treatment. Phospho-FGFR was significantly inhibited in SNU-16 tumor tissues 1 hour after a single oral dose of AZD4547 12.5 mg/kg and was partially restored 24 hours following treatment. D, pharmacokinetics and pharmacodynamics modeling in a SNU-16 xenograft model. AZD4547 12.5 mg/kg was administered by oral gavage to tumor-bearing nude mice; plasma and tumor xenografts were collected at various time points indicated after dosing. Total concentration of AZD4547 in plasma was plotted on the left axis, and phospho-Erk and phospho-PLCγ levels in xenografts were plotted on the right axis. IC_{50} and IC_{90} values of AZD4547 in an *in vitro* SNU-16 antiproliferation assay are also indicated. E, Ki67 IHC staining and TUNEL assay images of xenograft sections following treatment with a single dose of 12.5 mg/kg AZD4547. GAPDH, glyceraldehyde-3-phosphate dehydrogenase.

established SNU-16 xenografts led to tumor regression only in those tumors stably expressing tet-controlled *FGFR2* shRNA (clones 3C8 or 2B; Fig. 3A). Tumor regrowth was observed following cessation of doxycycline treatment (Fig. 3A).

Similarly, treatment of mice harboring *FGFR2*-amplified SNU-16 cells with AZD4547 over a 25-day period resulted in dose-dependent tumor growth inhibition (TGI), with significant tumor regression achieved using a daily dose of 12.5 mg/kg AZD4547 (Fig. 3B).

To assess pharmacodynamic effects, mice bearing SNU-16 xenografts were treated with a single oral dose of 12.5 mg/kg AZD4547. Two hours post-dose, greater than 95% inhibition of tumor FGFR2 phosphorylation was achieved, with partial recovery observed by Western blot analysis at 24 hours (Fig. 3C). Using both Western blot analysis and IHC approaches, levels of the downstream markers phospho-ERK and phospho-PLCγ were suppressed by 90% or more at 10 hours, with partial recovery apparent by 24 hours post-dose (Fig. 3D). The overall total plasma concentration of AZD4547 that was required to maintain 24-hour coverage of phospho-FGFR modulation correlated well with the AZD4547 concentration required for 90% inhibition (IC_{90}, 50 nmol/L) of SNU-16 cell growth in an *in vitro* antiproliferation assay. In addition, 50% inhibition of phospho-Erk and phospho-PLCγ was also observed at the AZD4547

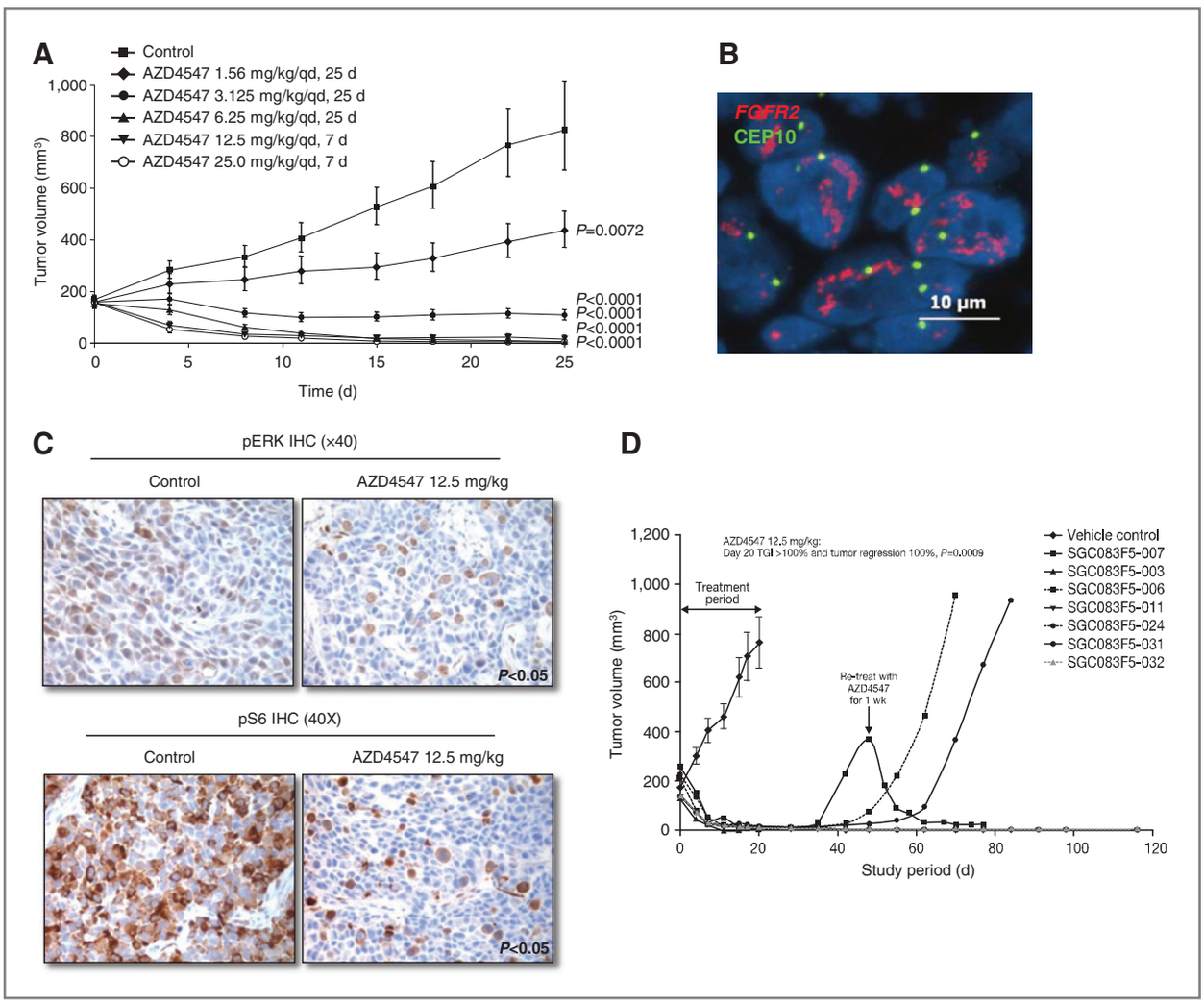

Figure 4. AZD4547 displays potent antitumor efficacy in a *FGFR2*-amplified PDGCX model. A, growth curve of model SGC083 treated with AZD4547. Tumor-bearing nude mice were treated daily for 7 to 25 days with AZD4547 (or vehicle) at concentrations indicated. Tumor volume was measured at the time indicated. Statistical analysis of TGI was conducted using a Student *t* test. B, FISH analysis of *FGFR2* gene copy number in model SGC083. Red signals represent *FGFR2* genes, whereas green signals represent *CEP10*. C, pharmacodynamics study of AZD4547 in model SGC083. IHC study of phospho-Erk and phospho-S6 (S240/244) after AZD4547 treatment. Pharmacodynamics data are from 2 hours following a single AZD4547 12.5 mg/kg dose after 25 days of dosing with AZD4547 1.56 mg/kg/once daily. D, rechallenge of FGFR2-amplified SGC083 PDTX models. AZD4547 was dosed daily for 20 days, after which it was withdrawn and complete regression maintained in 4 of 7 tumors to day 116. One of 3 tumors that progressed at day 35 was rechallenged with AZD4547 (12.5 mg/kg) at day 48 for 20 days; this xenograft remained sensitive to AZD4547. qd, once daily.

IC_{90} (50 nmol/L) concentration in the SNU-16 pharmacokinetics/pharmacodynamics tumor xenograft model (Fig. 3D).

Importantly, AZD4547 treatment led to a significant reduction in the proportion of SNU-16 tumor xenograft cells staining positive for Ki67 and an increase in those positive for apoptotic markers (Fig. 3E).

AZD4547 induces tumor regressions in a PDGCX model carrying *FGFR2* amplification

To extend the translational relevance of our findings, we next sought to identify and test AZD4547 in a relevant PDGCX model. FISH analysis identified the PDGCX model, SGC083, as being *FGFR2*-amplified (Fig. 4B). Antitumor efficacy studies confirmed this model to be highly sensitive and dose responsive to AZD4547 treatment, with significant tumor regression achieved using a daily 6.25 mg/kg dose of AZD4547 and complete tumor regression (undetectable tumors) was observed at doses of 12.5 and 25 mg/kg AZD4547 (Fig. 4A). Moreover, using quantified IHC staining, significant modulation ($P < 0.05$) of phospho-Erk and phospho-S6 was shown using a dose of 12.5 mg/kg AZD4547 (Fig. 4C), thus confirming pathway modulation *in vivo*.

In contrast to the marked tumor regressions observed upon AZD4547 treatment of the *FGFR2*-amplified SNU-16 and SGC083 xenograft models, only minimal to partial TGI was observed in the AZ521, MGC803, G001, and G009 *FGFR2* nonamplified gastric cancer xenograft models (Table 1). Furthermore, treatment of the *FGFR2* low polysomy model, G001, with 12.5 mg/kg AZD4547 did not result in significant modulation of pFGFR, pFRS2, or pErk (data not shown). Indeed, baseline expression of pFGFR2 and corresponding pathway activation were low or undetectable across the *FGFR2* nonamplified models we tested (data not shown).

To investigate the durability of the AZD4547 antitumor effect, mice bearing established SGC083 tumors were treated with 12.5 mg/kg AZD4547 for 20 days, at which point full tumor regression was achieved. Of 7 mice, 4 were still tumor free at day 116 when measurements were stopped. Three mice began to show tumor regrowth around day 35, thus providing the opportunity for drug rechallenge. One mouse (SGC083F5-007) was rechallenged with 12.5 mg/kg AZD4547 at day 48, and complete regression was reestablished after a further 20 days of treatment (Fig. 4D).

Combined treatment with AZD4547 enhances the antitumor efficacy of cytotoxic agents in the *FGFR2*-amplified SNU-16 xenograft model

To assess the effects of combining AZD4547 treatment with existing standard of care chemotherapies, the SNU-16 xenograft model was tested preclinically with 5-FU (10 mg/kg/once daily)/cisplatin (4 mg/kg/once weekly; FC) and a low dose of AZD4547 (3.1 mg/kg/once daily). Single-agent FC or AZD4547 gave TGI values of 25% and 34%, respectively, whereas 68% TGI was achieved when the same doses of AZD4547 and FC were combined (Fig. 5A). Similar results were observed when AZD4547 was combined with either docetaxel or irinotecan. Single-agent docetaxel treatment achieved 48% TGI, whereas the combination with AZD4547 resulted in approximately 82% TGI. Monotherapy usage of irinotecan or AZD4547 generated TGI values of 60% and 14%, respectively, whereas the combination resulted in significant tumor regression (100% TGI; Fig. 5B). The combination regimens were well tolerated as determined by minimal body weight loss (data not shown).

Table 1. Correlation between *FGFR2* gene amplification and sensitivity to AZD4547 in a range of standard and PDGCX xenograft models

		AZD4547 12.5 mg/kg	
Model	*FGFR2* status (by FISH)	TGI, %	Tumor regression, %
SNU-16	Amplified	>100	64[b]
AZ521	Disomy	63	—
MGC803	Disomy	37	—
SGC083[a]	Amplified	>100	90[c]
G001[a]	Polysomy	34	—
G009[a]	Trisomy	23	—

[a]PDGCX model.
[b]Tumor regression was assessed at the end of the study.
[c]AZD4547 was administered for 7 days and tumor regression was assessed on day 25 after first dose.

Discussion

Genetic aberrations of FGFR family members have been identified in different types of cancers. For example, *FGFR1* amplification has been observed in breast, ovarian, and lung cancer (31–33) and *FGFR3* mutation has been identified in bladder cancer (34). *FGFR2* genetic mutation or amplification leads to abnormal activation of the FGFR2 signaling pathway and contributes to carcinogenesis and tumor development in melanoma and gastric cancers, respectively (35–38). In this study, we report *FGFR2* gene amplification incidence rates of 4.5% and 7% in cohorts of Chinese and Caucasian patients with gastric cancer, respectively, consistent with previously published reports (36, 37). Interestingly, *FGFR2* amplification was found to be mutually exclusive with *HER2* and *c-MET* amplifications in these patient samples (data not shown). Thus, our data confirm the presence of a distinct segment of patients with gastric cancer harboring tumors molecularly characterized by *FGFR2* amplification, not only in the East Asian population, but also in Caucasian patients. The percentage of patients with gastric cancer who have *FGFR2* amplification is low at 5% to 7%, and hence identification of this cohort will present a significant challenge to the clinical development and treatment strategy. However, recent examples such as crizotinib in lung cancer (39) and trastuzumab in both breast and gastric cancer (40), show that in common

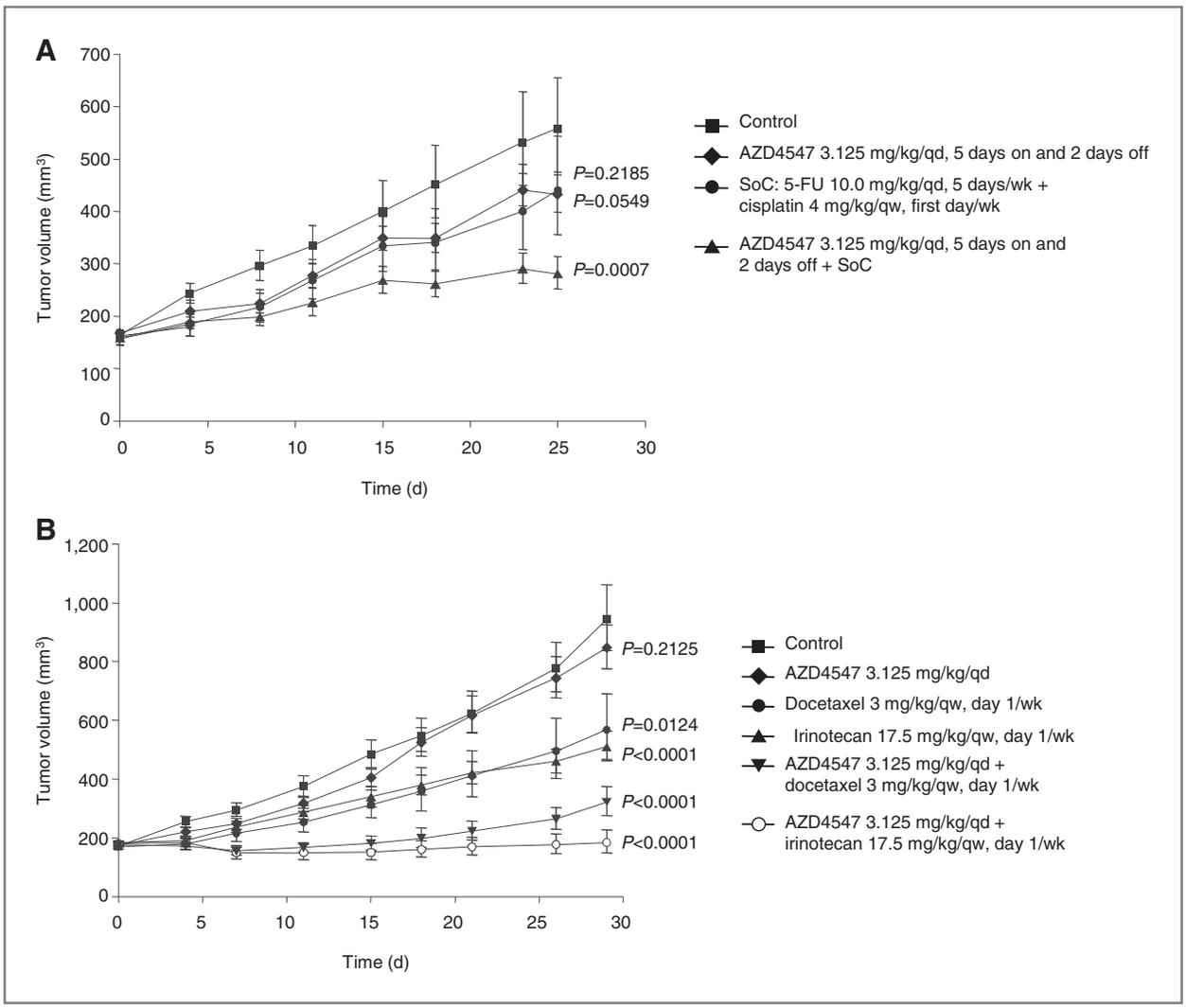

Figure 5. AZD4547 enhances the efficacy of cytotoxic agents in the SNU-16 *FGFR2*-amplified xenograft model. A, SNU-16 xenograft-bearing nude mice were treated with either vehicle, AZD4547 3.1 mg/kg or FC (5-FU 10 mg/kg and cisplatin 4 mg/kg) alone, or a combination of AZD4547 and FC as indicated. AZD4547 and 5-FU were administered in a 5 day on, 2 day off treatment schedule. Cisplatin was administered once weekly. Statistical analysis of TGI was conducted using a Student *t* test. B, AZD4547 enhanced the efficacy of docetaxel and irinotecan chemotherapy in the SNU-16 xenograft model. Statistical analysis of TGI was conducted using a Student *t* test. qd, once daily; qw, once weekly.

cancers niche patients can be identified and successfully treated by highly targeted drugs.

Two approaches were used to functionally inhibit FGFR2 in gastric cancer cell lines and patient-derived xenograft models; pharmacologic modulation with the small-molecule inhibitor AZD4547, and specific shRNA knockdown of the *FGFR2* gene. The results of these studies show that *FGFR2* gene amplification is an oncogenic driver in gastric cancer. Once-daily oral administration of AZD4547 or shRNA knockdown of *FGFR2* resulted in a rapid tumor regression in FGFR2-amplified models, and this was accompanied by inhibition of tumor phospho-FGFR2 levels and downstream signaling through phospho-PLCγ, phospho-Erk, and phospho-S6. At a dose sufficient to induce tumor regression in a *FGFR2*-amplified model, AZD4547 displayed complete inhibition of tumor phospho-FGFR2, phospho-Erk, and phospho-PLCγ for almost 24 hours. Indeed, the total AZD4547 *in vivo* drug exposure was maintained above the level required for complete *in vitro* inhibition of phospho-PLCγ and phospho-Erk and the antiproliferation IC_{90} value in the SNU-16 cell line. Furthermore, antitumor efficacy was accompanied by inhibition of tumor Ki67 staining and induction of apoptosis. AZD4547 treatment did not, however, result in pharmacodynamics modulation of FGFR or downstream markers in a *FGFR2* nonamplified xenograft model (G001). These data together suggest that AZD4547 exerts potent antitumor efficacy through direct inhibition of pFGFR2, with resulting pharmacodynamics pathway modulation only in those models with amplified *FGFR2*.

Chemotherapy regimens are commonly used in gastric cancer, including cisplatin/5-FU doublet therapy in first line and taxane or irinotecan monotherapy for second-line disease. Here, we have shown that AZD4547 can be combined with these chemotherapies in the SNU16 FGFR2-amplified model, resulting in antitumor efficacy greater than that achieved with either AZD4547 monotherapy or chemotherapy alone. Although these studies provide preliminary evidence for the feasibility of combining AZD4547 with chemotherapies, further studies are required to investigate the mechanistic interactions between AZD4547 and these standards of care.

Compared with standard cell line–derived tumor xenografts, PDGCX models offer the benefits of more informative disease models through maintenance of tumor heterogeneity and preservation of tumor architecture. Importantly, the *FGFR2* amplification status was maintained between the PDGCX models used and the original patient tumor samples from which they were derived (data not shown). Interestingly, we were able to conduct some limited investigation of the rates and durability of complete tumor regression using the PDGCX model, SGC083. Following once-daily dosing of 12.5 mg/kg AZD4547, all 7 mice showed complete regression of tumors within 3 weeks, and importantly, 4 of the mice were still tumor free at the end of the study on day 116. Of the 3 tumors, which regrew, 1 was rechallenged with AZD4547 and regression reestablished, indicating that the tumor remained sensitive to FGFR2 inhibition and that FGFR2 was likely still the "driver" oncogene within this tumor. To our knowledge, this is the first observation of a *FGFR2*-amplified PDGCX tumor model showing such robust and durable antitumor response to a targeted pharmacologic agent. Taken together, the studies above show that *FGFR2* amplification leads to constitutive activation of the FGFR2 signaling pathway in gastric cancer, and furthermore that inhibition of this pathway using a well-tolerated, potent, and selective inhibitor can lead to rapid and durable tumor regressions in *FGFR2*-amplified gastric cancer xenograft models.

In summary, our data show the existence of a cohort of Chinese and Caucasian patients with gastric cancer harboring *FGFR2* gene amplification. Moreover, we have shown the dependency of activated FGFR2 and downstream signaling on gastric cancer growth and survival *in vitro* and *in vivo*, using selective *FGFR2* shRNA and the FGFR inhibitor, AZD4547. Thus, the preclinical data reported here support further development of FGFR inhibitors, such as AZD4547, as potential therapeutic agents for the treatment of patients with *FGFR2*-amplified gastric cancer.

Disclosure of Potential Conflicts of Interest

Y. Xu is employed as Senior Associate Scientist in AstraZeneca. X. Zhang is the Vice President of AstraZeneca. No potential conflicts of interest were disclosed by the other authors.

Authors' Contributions

Conception and design: L. Xie, M. Zhou, D. Shen, J. Zhang, E. Kilgour, X. Zhang, Q. Ji

Development of methodology: L. Xie, X. Su, L. Zhang, X. Yin, L. Tang, Y. Xu, K. Liu

Acquisition of data (provided animals, acquired and managed patients, provided facilities, etc.): L. Xie, X. Su, L. Zhang, L. Tang, X. Zhang, Y. Xu, K. Liu, B. Gao, L. Zhang, J. Ji

Analysis and interpretation of data (e.g., statistical analysis, biostatistics, computational analysis): L. Xie, X. Yin, Z. Gao, P.R. Gavine, E. Kilgour, X. Zhang, Q. Ji

Writing, review, and/or revision of the manuscript: L. Xie, X. Su, L. Zhang, X. Yin, Z. Gao, P.R. Gavine, E. Kilgour, Q. Ji

Administrative, technical, or material support (i.e., reporting or organizing data, constructing databases): L. Xie, X. Su, L. Zhang, X. Yin, L. Zhang, J. Ji

Study supervision: L. Xie, B. Gao, J. Zhang, X. Zhang, Q. Ji

Acknowledgments

The authors thank Yao Wang, Min Shi, Katherine Ye, Zengquan Wang for data generation; Jie Zang for drafting the article.

Grant Support

This study was sponsored by AstraZeneca. Editorial assistance was provided by Claire Routley from Mudskipper Bioscience, funded by AstraZeneca.

The costs of publication of this article were defrayed in part by the payment of page charges. This article must therefore be hereby marked *advertisement* in accordance with 18 U.S.C. Section 1734 solely to indicate this fact.

Received December 21, 2012; revised February 14, 2013; accepted February 28, 2013; published OnlineFirst March 14, 2013.

References

1. Jemal A, Bray F, Center MM, Ferlay J, Ward E, Forman D. Global cancer statistics. CA Cancer J Clin 2011;61:69–90.
2. Naylor GM, Gotoda T, Dixon M, Shimoda T, Gatta L, Owen R, et al. Why does Japan have a high incidence of gastric cancer? Comparison of gastritis between UK and Japanese patients. Gut 2006;55:1545–52.
3. Parkin DM. The global health burden of infection-associated cancers in the year 2002. Int J Cancer 2006;118:3030–44.
4. Roukos DH. Targeting gastric cancer with trastuzumab: new clinical practice and innovative developments to overcome resistance. Ann Surg Oncol 2010;17:14–7.
5. Mlkvy P. Multimodal therapy of gastric cancer. Dig Dis 2010;28:615–8.
6. Hanahan D, Weinberg RA. Hallmarks of cancer: the next generation. Cell 2011;144:646–74.
7. Gorringe KL, Boussioutas A, Bowtell DD. Novel regions of chromosomal amplification at 6p21, 5p13, and 12q14 in gastric cancer identified by array comparative genomic hybridization. Genes Chromosomes Cancer 2005;42:247–59.
8. Stuart D, Sellers WR. Linking somatic genetic alterations in cancer to therapeutics. Curr Opin Cell Biol 2009;21:304–10.
9. Gazdar AF, Shigematsu H, Herz J, Minna JD. Mutations and addiction to EGFR: the Achilles 'heal' of lung cancers? Trends Mol Med 2004;10:481–6.
10. Soda M, Choi YL, Enomoto M, Takada S, Yamashita Y, Ishikawa S, et al. Identification of the transforming EML4-ALK fusion gene in non–small-cell lung cancer. Nature 2007;448:561–6.
11. Greenman C, Stephens P, Smith R, Dalgliesh GL, Hunter C, Bignell G, et al. Patterns of somatic mutation in human cancer genomes. Nature 2007;446:153–8.
12. Buffart TE, Louw M, van Grieken NC, Tijssen M, Carvalho B, Ylstra B, et al. Gastric cancers of Western European and African patients show

different patterns of genomic instability. BMC Med Genomics 2011;4:7.
13. Janjigian YY, Tang LH, Coit DG, Kelsen DP, Francone TD, Weiser MR, et al. MET expression and amplification in patients with localized gastric cancer. Cancer Epidemiol Biomarkers Prev 2011;20:1021–7.
14. Jin K, He K, Han N, Li G, Wang H, Xu Z, et al. Establishment of a PDTT xenograft model of gastric carcinoma and its application in personalized therapeutic regimen selection. Hepatogastroenterology 2011;58: 1814–22.
15. Fan B, Dachrut S, Coral H, Yuen ST, Chu KM, Law S, et al. Integration of DNA copy number alterations and transcriptional expression analysis in human gastric cancer. PLoS ONE 2012;7:e29824.
16. Deng N, Goh LK, Wang H, Das K, Tao J, Tan IB, et al. A comprehensive survey of genomic alterations in gastric cancer reveals systematic patterns of molecular exclusivity and co-occurrence among distinct therapeutic targets. Gut 2012;61:673–84.
17. Eswarakumar VP, Lax I, Schlessinger J. Cellular signaling by fibroblast growth factor receptors. Cytokine Growth Factor Rev 2005;16:139–49.
18. Fukumoto S. Actions and mode of actions of FGF19 subfamily members. Endocr J 2008;55:23–31.
19. Brooks AN, Kilgour E, Smith PD. Molecular pathways: fibroblast growth factor signaling: a new therapeutic opportunity in cancer. Clin Cancer Res 2012;18:1855–62.
20. Katoh M, Katoh M. FGF signaling network in the gastrointestinal tract (review). Int J Oncol 2006;29:163–8.
21. Katoh M. Genetic alterations of FGF receptors: an emerging field in clinical cancer diagnostics and therapeutics. Expert Rev Anticancer Ther 2010;10:1375–9.
22. Grose R, Dickson C. Fibroblast growth factor signaling in tumorigenesis. Cytokine Growth Factor Rev 2005;16:179–86.
23. Jang JH, Shin KH, Park JG. Mutations in fibroblast growth factor receptor 2 and fibroblast growth factor receptor 3 genes associated with human gastric and colorectal cancers. Cancer Res 2001;61: 3541–3.
24. Davies H, Hunter C, Smith R, Stephens P, Greenman C, Bignell G, et al. Somatic mutations of the protein kinase gene family in human lung cancer. Cancer Res 2005;65:7591–5.
25. Stephens P, Edkins S, Davies H, Greenman C, Cox C, Hunter C, et al. A screen of the complete protein kinase gene family identifies diverse patterns of somatic mutations in human breast cancer. Nat Genet 2005;37:590–2.
26. Bai A, Meetze K, Vo NY, Kollipara S, Mazsa EK, Winston WM, et al. GP369, an FGFR2-IIIb-specific antibody, exhibits potent antitumor activity against human cancers driven by activated FGFR2 signaling. Cancer Res 2010;70:7630–9.
27. Kilgour E, Su X, Zhan P, Gavine P, Morgan S, Womack C, et al. Prevalence and prognostic significance of FGF receptor 2 (*FGFR2*) gene amplification in Caucasian and Korean gastric cancer cohorts. J Clin Oncol 30, 2012 (suppl; abstr 4124).
28. Beenken A, Mohammadi M. The FGF family: biology, pathophysiology and therapy. Nat Rev Drug Discov 2009;8:235–53.
29. Gavine PR, Mooney L, Kilgour E, Thomas AP, Al-Kadhimi K, Beck S, et al. AZD4547: an orally bioavailable, potent, and selective inhibitor of the fibroblast growth factor receptor tyrosine kinase family. Cancer Res 2012;72:2045–56.
30. Liehr T (Ed.). Fluorescence *in situ* hybridization (FISH) application guide. Springer; 2009. ISBN 978-3-540-70581-9.
31. Theillet C, Adelaide J, Louason G, Bonnet-Dorion F, Jacquemier J, Adnane J, et al. FGFRI and PLAT genes and DNA amplification at 8p12 in breast and ovarian cancers. Genes Chromosomes Cancer 1993;7: 219–26.
32. Turner N, Pearson A, Sharpe R, Lambros M, Geyer F, Lopez-Garcia MA, et al. FGFR1 amplification drives endocrine therapy resistance and is a therapeutic target in breast cancer. Cancer Res 2010;70: 2085–94.
33. Weiss J, Sos ML, Seidel D, Peifer M, Zander T, Heuckmann JM, et al. Frequent and focal FGFR1 amplification associates with therapeutically tractable FGFR1 dependency in squamous cell lung cancer. Sci Transl Med 2010;2:62ra93.
34. Turner N, Grose R. Fibroblast growth factor signalling: from development to cancer. Nat Rev Cancer 2010;10:116–29.
35. Gartside MG, Chen H, Ibrahimi OA, Byron SA, Curtis AV, Wellens CL, et al. Loss-of-function fibroblast growth factor receptor-2 mutations in melanoma. Mol Cancer Res 2009;7:41–54.
36. Jung EJ, Jung EJ, Min SY, Kim MA, Kim WH. Fibroblast growth factor receptor 2 gene amplification status and its clinicopathologic significance in gastric carcinoma. Hum Pathol 2012;43:1559–66.
37. Matsumoto K, Arao T, Hamaguchi T, Shimada Y, Kato K, Oda I, et al. FGFR2 gene amplification and clinicopathological features in gastric cancer. Br J Cancer 2012;106:727–32.
38. Moffa AB, Tannheimer SL, Ethier SP. Transforming potential of alternatively spliced variants of fibroblast growth factor receptor 2 in human mammary epithelial cells. Mol Cancer Res 2004;2: 643–52.
39. Gandhi L, Janne PA. Crizotinib for ALK-rearranged non–small cell lung cancer: a new targeted therapy for a new target. Clin Cancer Res 2012;18:3737–42.
40. Lordick F. Trastuzumab: a new treatment option for HER2-positive metastatic gastric and gastroesophageal junction cancer. Future Oncol 2011;7:187–99.